

Development of Computer Code for Simulation of Multicomponent Aerosol Dynamics

—Uncertainty and Sensitivity Analysis—

Jang Hwan Na and Byong Whi Lee

Korea Advanced Institute of Science and Technology

(Received February 16, 1987)

다성분 에어로졸계의 동특성 묘사를 위한 전산 코드의 개발

—불확실성 및 민감도 해석—

나 장 환 · 이 병 휘

한국과학기술원

(1987. 2. 16 접수)

Abstract

To analyze the aerosol dynamics in severe accidents of LMFBR, a new computer code entitled MCAD (Multicomponent Aerosol Dynamics) has been developed. The code can treat two component aerosol system using relative collision probability of each particles as sequences of accident scenarios.

Coagulation and removal mechanisms incorporating Brownian diffusion and gravitational sedimentation are included in this model. In order to see the effect of particle geometry, the code makes use of the concept of density correction factor and shape factors.

The code is verified using the experimental result of NSPP-300 series and compared to other code. At present, it fits the result of experiment well and agrees to the existing code.

The input variables included are very uncertain. Hence, it requires uncertainty and sensitivity analysis as a supplement to code development. In this analysis, 14 variables are selected to analyze. The input variables are compounded by experimental design method and Latin hypercube sampling. Their results are applied to Response surface method to see the degree of regression. The stepwise regression method gives an insight to which variables are significant as time elapse and their reasonable ranges. Using Monte Carlo Method to the regression model of LHS, the confidence level of the results of MCAD and their variables is improved.

요 약

중대사고시 LMFBR의 에어로졸(aerosol) 동특성을 살피기 위해 전산코드인 MCAD(Multicomponent Aerosol Dynamics)가 개발되었다. 사고경과에 따른 두 방사능원의 상대적인 충돌확률을 적용하여 에어로졸계를 묘사할 수 있다.

Brownian 확산과 중력작용에 의한 결함 및 제거과정을 고려했으며, 입자형태를 묘사하기 위해 밀도보정과 형태요소(shape factor)를 동시에 고려하였다.

ORNL의 NSPP-300 계열 실험자료와 기존의 코드를 MCAD의 입증에 이용하였다. 그 결과 MCAD의 계산치와 실험치 및 기존의 코드 계산값이 일치함을 보여준다.

여러 입력자료의 불확실한 값들을 정의하고, 그들값의 한계로 설정하기 위하여 불확실성 및 민감도해석을 수행하였다. 14개의 입력자료를 선택하여 실험계획법과 Latin hypercube sampling에 의한 입력자료를 조합하여 그 회귀(regression) 정도를 반응표면 계획법(Response surface method)에 의해 구하였다.

각 변수들의 중요성 및 시간경과에 따른 그들의 상대적인 등위를 결정하기 위하여 단계식 회귀방법(Stepwise regression method)을 고려했다.

LHS에 의한 회귀모형에 Monte Carlo Method를 적용하여 계산값 및 변수들에의 신뢰도를 향상시켰다.

Nomenclatures

Alphabets

A	: Area of containment wall or floor
$Bc(s)$: Brownian coagulation coefficient where Bs is in $Kn < 0.25$
Br	: Brownian diffusional deposition
B_i	: Regression coefficient
C_f	: Slip correction factor
D	: Particle diameter
F_i	: Partial correlation coefficient
Gc	: Gravitational coagulation coefficient
Gr	: Gravitational sedimentation
Kn	: Knudsen number
K	: Boltzmann constant
Lr	: Leakage removal rate
$n(u, t)$: Number concentration of particle having mass u
P	: Pressure
Q_{lk}	: Particle mass concentration of section l and component k where Q_l is integrated quantity of section l
R_{lk}	: Removal rate
S_{lk}	: Source rate
Tc	: Turbulent coagulation coefficient
Tr	: Thermophoresis removal
T	: Temperature
t	: Time
V	: Containment volume
$Vu(v)$: Mean velocity of particle $u(v)$
$Vsu(v)$: Sedimentation velocity of particle $u(v)$

u, v	: Particle mass where Q is nv
Y	: Results by computer run
\hat{Y}	: Response by regression model

Greeks

α	: Sticking probability factor
β	: Coagulation coefficient of between u and v
γ	: Agglomeration shape factor
δ	: Diffusion boundary layer thickness
ϵ	: Turbulence dissipation rate
η	: Viscosity
κ	: Ratio of thermal conductivity gas to particle
λ	: Mean free path of medium
ρ	: Particle density
ρ_g	: gas (Here, air) density
χ	: Dynamic shape factor
ψ	: Diffusion coefficient
θ	: Delta function

Subscripts

l	: Number of sections ($1, \dots, M$)
k	: Particle classes ($1, \dots, K$)
c	: Coagulation coefficient
r	: Removal rate
i	: Variable to identify the particle mass u or v

I. Introduction

During the Three Mile Island accident in 1979, only a trace amount of radioiodine was released to the environment. This significant

discrepancy between the actual release and the expected WASH-1400 study¹⁾ raised questions why such a large differences existed. In 1980, it was clearly demonstrated that the only small amount of radioactivity release to the environment would be made in such an accident scenarios.²⁾ While, TMI appears to be a partial meltdown of fuel accident, some of the previous accident experiments which had undergone significant fuel degradation also resulted in a much smaller amount of radioactivity release to the environment even though most of the reactors, unlike TMI, were not confined in containment buildings.

As a result of these observations, a number of new studies reexamining the WASH-1400 methodology and experimental research programmes were started.^{3),4)}

Summing up these results, two phenomena are remarkable to explain on the reduction of source term. These are chemical and physical mechanisms of aerosol particles. In this paper, only physical mechanisms of aerosol particles are surveyed.

In the study of nuclear aerosols in severe accidents, much effort has been devoted to homogeneous aerosol as a spatially independent, single components model, such as HAARM-3.⁵⁾ But, this situation is unsatisfactory in some cases when various materials are generated at different times and with different size distributions. Thus, the multicomponent aerosol models incorporating the composition are necessary to analyze the real accident conditions.

Consequently, such computer codes as MSPEC⁶⁾ which is an extension of single component model of QUICK and MAEROS⁷⁾ were developed several years ago at Battelle Columbus Lab. and Sandia National Lab. respectively.

Although simplified assumptions are adopted, the codes have inherent uncertainties which have order of magnitude and complication. Also, their uncertainty and sensitivity analysis gives a large

differences in input variable range. These variables make it difficult to approach analytical analysis of multicomponent model which is more complicated than a single component model.

Therefore, it would be desirable to develop a more simplified aerosol behavior model which is conservative and have concise input variables. Also, the code have to accept three or more component system which can be a major factor of confidence of analysis. This necessity is accentuated by the fact that the complexity and cost of experiment prohibited the application of more realistic situation.

In the present work, a new computer code entitled MCAD (Multicomponent Aerosol Dynamics) has been developed. The mathematical model used in MCAD is briefly described and numerical approach to its solution is discussed. The code is verified using the results of NSPP-300 series experiments¹⁰⁾ carried out at Oak Ridge National Lab. (ORNL) and MSPEC code. The present study includes uncertainty and sensitivity analysis to identify variable uncertainty and sensitivity of the code.

II. Mathematical Modeling

Governing Equation

A general mathematical model of the aerosol dynamics is approached. The physical phenomena in the model are based on coagulation, source and removal mechanisms.

A dynamic equation for treating the multicomponent aerosol is derived by F. Gelbard et al.⁹⁾

$$\begin{aligned} \frac{dQ_{ik}}{dt} = & \frac{1}{2} \sum_{i=1}^{l-1} \sum_{j=1}^{l-1} (\bar{\beta}_{i,j}^{1a} Q_{i,j} Q_{i,k} + \bar{\beta}_{i,j}^{1b} Q_{i,j} Q_{i,k}) \\ & - \sum_{i=1}^{l-1} (\bar{\beta}_{i,i}^{2a} Q_i Q_{i,k} - \bar{\beta}_{i,i}^{2b} Q_i Q_{i,k}) \\ & - \frac{1}{2} \bar{\beta}_{i,i}^3 Q_i Q_{i,k} - Q_{i,k} \sum_{i=1}^m \bar{\beta}_{i,i}^4 Q_i \\ & + S_{i,k} - \bar{R}_{i,k} \end{aligned} \quad (1)$$

Table 1. Sectional Coefficient of Eq. II. (1)

1) Coagulation			
1a	$\bar{\beta}_{ijl}$	$1 < l \leq m$	$\int_{x_{l-1}}^{x_i} \int_{x_{j-1}}^{x_l} \frac{\theta(v_{l-1} < u+v < v_l) u \beta(u, v)}{uv(x_i - x_{i-1})(x_j - x_{j-1})} dy dx$
		$1 \leq i < l$	
		$1 \leq j < l$	
1b	$\bar{\beta}_{ijl}$	$1 < l \leq m$	$\int_{x_{l-1}}^{x_i} \int_{x_{j-1}}^{x_l} \frac{\theta(v_{l-1} < u+v < v_l) v \beta(u, v)}{uv(x_i - x_{i-1})(x_j - x_{j-1})} dy dx$
		$1 \leq i < l$	
		$1 \leq j < l$	
2a	$\bar{\beta}_{il}$	$1 < l \leq m$	$\int_{x_{l-1}}^{x_i} \int_{x_{l-1}}^{x_l} \frac{\theta(u+v > v_l) u \beta(u, v)}{uv(x_i - x_{i-1})(x_l - x_{l-1})} dy dx$
		$1 \leq i < l$	
2b	$\bar{\beta}_{il}$	$1 < l \leq m$	$\int_{x_{l-1}}^{x_i} \int_{x_{l-1}}^{x_l} \frac{\theta(v+u < v_l) v \beta(u, v)}{uv(x_i - x_{i-1})(x_l - x_{l-1})} dy dx$
		$1 \leq i < l$	
3	$\bar{\beta}_{il}$	$1 \leq l \leq m$	$\int_{x_{l-1}}^{x_i} \int_{x_{l-1}}^{x_l} \frac{\theta(u+v > v_l) (u+v) \beta(u, v)}{uv(x_i - x_{i-1})(x_l - x_{l-1})} dy dx$
4	$\bar{\beta}_{il}$	$1 \leq l < m$ $1 < i \leq m$	$\int_{x_{l-1}}^{x_i} \int_{x_{l-1}}^{x_l} \frac{u \beta(u, v)}{uv(x_i - x_{i-1})(x_l - x_{l-1})} dy dx$
2) Source			
	\bar{S}_{lk}	$1 \leq l \leq m$	$\int_{v_{l-1}}^{u_l} V_k S(v_k, t) dv$
3) Removal			
	\bar{R}_{lk}	$1 \leq l \leq m$	$Q_{lk} \int_{x_{l-1}}^{x_l} \frac{R(v, t)}{(x_l - x_{l-1})} dx$

$$x_i = f(v_i), u = f^{-1}(y), v = f^{-1}(x)$$

Table 1 gives the coefficients of Eq. (1).

Coagulation Coefficient

Coagulation is used to describe the process of adhesion or fusion of aerosol particles upon contact with one another. The growth by agglomeration is specially significant because particle size is a critically important factor in aerosol dynamic behavior.

The three dominant mechanisms that make up the collision kernel are assumed to be separable and additive. The overall coagulation coefficient $C(u, v)$ is represented by

$$C(u, v) = Bc(u, v) + Gc(u, v) + Tc(u, v) \quad (2)$$

where $Bc(u, v)$ refers to brownian coagulation, $Gc(u, v)$ to gravitational coagulation and $Tc(u, v)$ to turbulent coagulation.

Brownian coagulation results from the random motion of aerosols by collisions with gas molecules. It may be divided by Knudsen Number, $Kn = 2\lambda_g/D$. Here λ_g is mean free path of medium and D is particle diameter. The difference in sedimentation rates of particles due to different

sizes results in the larger one catches up the other. Turbulent coagulation results from random turbulent motion of the gas. Table 2 shows the three mechanisms of coagulation.

Removal Terms

Aerosols suspended in a containment vessel or any other buildings may deposit by a several mechanisms. These depend on the flow conditions, temperature distribution inside the containment vessel, gradient near the wall and containment geometry as well. Deposition rate $R(u)$ for aerosols in containment is the sum of individual rate, as

$$R(u) = Br(u) + Gr(u) + Tr(u) + Lr(u) \quad (3)$$

where $Br(u)$ refers to diffusion(brownian) deposition, $Gr(u)$ to gravitational sedimentation, $Tr(u)$ to thermophoresis and $Lr(u)$ to leakage removal rate.

The removal of aerosols by diffusion is given by Fick's law. Deposition onto floor or other horizontal planes occurs as a result of gravitational settling of particles. Aerosols suspended in

Table 2.1 Brownian Coagulation Coefficient $Bc(u, v)$

$Kn < 0.25$	$0.25 < Kn < 10$	$Kn > 10$
$Bs(u, v) = 2\pi(Du + Dv)^{11)}$ $(C_u\phi u + C_v\phi v)$ $\phi i = KT / (3\pi Di\eta\chi)$ $C_f = 1 + Kn(1.257 + 0.4^{12)})$ $\exp(-1.1/Kn)$	$Bc(u, v) = Bs(u, v) / Fuv^{13)}$ $Fuv = (Du + Dv) / (Du + Dv + 2Guv) + 8(\phi u + \phi v)$ $((Du + Dv)\alpha Vuv)$ $Guv = (GuGu + GvGv)^{1/2}$ $Gi = [(Di + Li)^3 - (Di^2 + Li^2)^{3/2}] / (3DiLi) - Di$ $Li = 8 \phi i / (\pi Vi)$	$Bc(u, v) = \pi(Du + Dv)^2 Vuv\alpha / 4$ $Vuv = (Vu^2 + Vv^2)^{1/2}$ $Vu = (8KT / \pi u)^{1/2}$

Table 2.2. Gravitational Coagulation Coefficient $Gc(u, v)$

$Gc(u, v) = Sg(Du, Dv) Vsu - Vsv $ $Vsi = \rho Di^2 Cfg / (18\eta\chi)$ Spherical Particle ¹⁴⁾ $Sg(Du, Dv) = \pi(Du + Dv)^2 Es(Du, Dv) / 4$ $Es(Du, Dv) = 1.5 [\text{Min}(Du, Dv) / (Du + Dv)]^2$ Nonspherical Particle ¹⁵⁾ $Sg(Du, Dv) = \pi(Du + Dv)^2 \times En(Du, Dv) / 4$ $En(Du, Dv) = Es(Du, Dv) \alpha \gamma^2$
--

Table 2.3. Turbulent Coagulation Coefficient $Tc(u, v)$

$Tc(u, v) = T_{1uv} + T_{2uv}^{16)}$ T_{1uv} (shear flow) $T_{1uv} = (\pi \epsilon \rho_g / 120\eta)^{1/2} \gamma^3 (Du + Dv)^3$ T_{2uv} (inertial force) $T_{2uv} = 0.074 Vsu - Vsv \gamma^2 (Du + Dv)^2 (\rho_g \epsilon^3 / \eta)^{1/2}$

Table 3. Removal Terms $R(u)$

Brownian	Gravitational	Thermophoresis
Diffusion	Sedimentation	$Tr(u) = (A/V) 3\gamma C_f^{(8)}$ $\Delta T (CtKn + \kappa) / Kt$
$Br(u) = (A/V) \phi u / \delta$	$Gr(u) = (A/V) Vsu$	$Kt = 2\chi \rho_g T (1 + 4.11 \times Kn) [1 + 2(CtKn + \kappa)]$

a gas experience a force toward cooler temperature if the gas exhibits a temperature gradient. The removal coefficients are given in Table 3.

Finally, the model does not consider leakage rate. That is, no containment breakage is assumed.

Source Term

These terms can be an arbitrary function of

time or others. Present model assumes constant rate of source generation during the release duration. For approximate analysis, the particle mass distribution on diameter is assumed to be lognormal.¹⁷⁾ Thus only total mass rate, lower and upper bounds of section, mass median diameter and geometric standard deviation are required in inputs.

Numerical Scheme

To solve the governing Eq.(1), Hamming's modified Predictor-Corrector method¹⁸⁾ is utilized. It is a general purpose function that solves a system of n first order ordinary differential equation. For accurate calculation of coagulation coefficient, double integral of a lengthy parameter is required. In multicomponent system, this is quite complicate, and following simplification is applied. If sectionalization is reasonably defined, the variation of coagulation coefficient between adjacent sections may be small, therefore $\beta(u, v)$ can be treated as constant in such a small interval.⁸⁾ In other words, convert the Eq. $\bar{\beta}_{ijl}$ in table 1, the final form given by

$$\beta(u, v) \theta(v_{l-1} < u + v < v_l) (u + v) / uv \quad (4)$$

where u and v are their representative values of particle range, and approximated by multiplying the relative collision probability

$$R_k = \beta_k(u, v) / \sum_{k=1}^2 \beta_k(u, v) \quad (5)$$

This approximation has not been sufficiently defined. However, considering that the coagula-

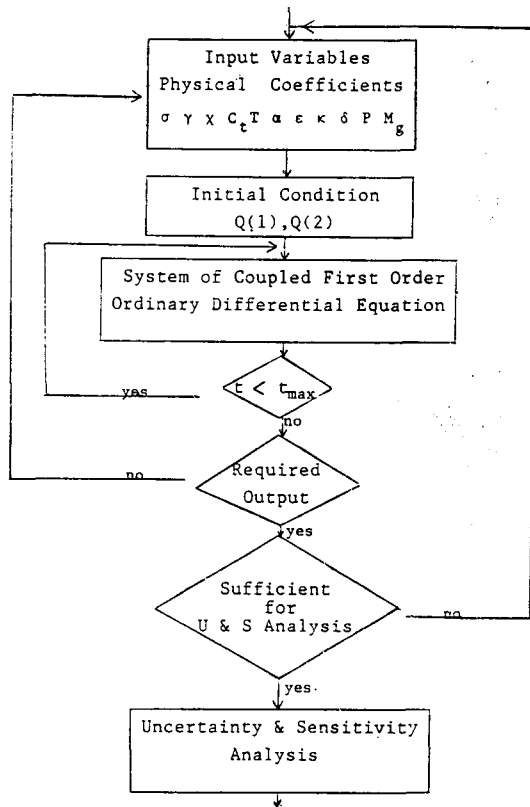


Fig. 1. Flow Diagram MCAD and its Analysis

tion coefficient depends on the mass of interacting particle, above assumption has its legitimacy. Accordingly, only particle size classification and Delta function are used. The simplicity and

usefulness can compensate for uncertainty due to assumption. In calculating the coagulation coefficient process of balance equation in each step, geometric constraints are applied to reduce time consuming. Geometric constraints are also contributed in avoiding the numerical error. That is, if small particles are encountered to larger ones, there is no mass change in interparticle sections. But, it raises a difficulty in treating Eq. (5).

In Fig. 1, main flow diagram and sensitivity analysis procedure are shown.

III. Uncertainty and Sensitivity Analysis

First, the required variables used in analysis are selected and simple data points can be assembled for code running. Table 4 shows the important input variables and their ranges also. Input variables be normalized for the stability of regression model.

Experimental Design Method¹⁰⁾

Experimental design method (EDM) requires the concept of level and resolution. The level is used for denoting the number of discrete values that a variable has. And, the resolution is related to the number of runs. Usually, two or three

Table 4. Variables Used in MCAD and Sensitivity Analysis

Order	Variable	Definition	Range
1	GSD	Geometric Standard Deviation of First and Second Component	1.5~2.5
2	GMD(1)	Geometric Mass Median Diameter of First Component (m)	0.5~1.0×10 ⁻⁶
3	GMD(2)	Geometric Mass Median Diameter of Second Component (m)	1.0~1.5×10 ⁻⁶
4	γ	Collision Shape Factor	1.5~2.0
5	χ	Dynamic Shape Factor	1.0~1.5
6	α	Sticking Probability Factor	0.5~1.0
7	δ	Diffusion Boundary Layer Thickness (m)	0.5~5.0×10 ⁻⁸
8	ϵ	Turbulence Dissipation Rate (m ² /s ³)	0.1~1.0×10 ⁻²
9	T	Temperature (K)	350~450
10	P	Pressure (Pa)	.96~1.0×10 ⁶
11	ΔT	Temperature Gradient (K/m)	3.0~5.0×10 ³
12	κ	Ratio of Thermal Conductivity of Gas to Particle	0.1~0.7
13	M_g	Molecular Weight of Gas (Kg/Kg. Mole)	20.~30.
14	C_t	Thermal Accomodation constant	1.0~2.0

level is utilized and related resolution will be used. In case of two level design, extreme variable range of -1 and 1 are taken and it is used for linear regression. If this method can not correlate the linear regression, three level design will be approached. In this case, the data points are -1 , 0 and 1 . The data points are selected by Placket-Burman method and central composite design which are part of partial factorial design.

Latin Hypercube Sampling²⁰⁾

In Latin hypercube sampling(LHS), the input variable X_k are partitioned into equal probability. The partitioned variables X_{ki} are combined randomly. LHS is advantageous when the output Y are dominated by only a few components of X_k . Therefore, this method will be pursued only when EDM is finished and important variables affecting to the code output are selected.

Response Surface Method²¹⁾

A correlation used in response surface method (RSM) is given as following form;

$$Y_j = f(X_1, X_2, \dots, X_k)_j \quad (6)$$

where X_k are input variables and Y_j are the results of correlations. In this paper, two level linear regression model is generated by multiple least square fitting by

$$\hat{Y} = B_0 + \sum_i B_i X_i \quad (7)$$

where B_i : regression coefficient which is constant
 \hat{Y} : response.

To see the difference of the output of code runs Y_j and response \hat{Y}_j , an estimator R^2 is introduced which is between 0 and 1 ,

$$R^2 = \sum_j (\hat{Y}_j - \bar{Y})^2 / \sum_j (Y_j - \bar{Y})^2 \quad (8)$$

where \bar{Y} is an average value of Y_j

Stepwise Regression Method²²⁾

Following will be directed to find the more important variables or the less. This can be obtained by applying stepwise regression method. At step one, the variable having the highest partial correlation coefficient (PCC) being taken where the coefficient given by

$$F_i = B_i^2 / ((X^T X)^{-1}_{ii} \text{mse}) \quad (9)$$

where mse is mean square error of the estimators as a measure of accuracy. Of the remaining variables, they are added successively on their contribution to the result of code. This calculation must be repeated until satisfactory R^2 value be achieved or PCC is less than the critical F distribution value.

Monte Carlo Method

Monte Carlo Method (MCM) is powerful in efficiency but time consuming because a lot of code runs are required to analyze the data values. Therefore, instead of direct method, MCM is applied to the regression model of EDM or LHS.

IV. Results and Discussion

Code Verification

Basically, the code verification requires experimental measurements and analytical studies. But, only limited experiments were executed. Therefore, best-fit experiments are not available in this case. Among the series of ORNL NSPP-300 experiments, #305 and #306 tests are adopted to verify the MCAD code. Table 5 shows input data in each experiment.

As shown in Table 2 and 3, the physical phenomena treated in MCAD are coagulation and removal mechanisms. The range of particle size used in the model is between 0.1 and 100 micrometer. In this range, gravitational and turbulent coagulation are more significant than Brownian

Table 5. NSPP-300 Series Experimental Data

Experiment	NSPP # 305		NSPP # 306	
Val. \ Comp.	U ₃ O ₈	Na ₂ O	U ₃ O ₈	Na ₂ O
Total Released Mass(KG)	0.165	1.281	0.151	1.65
Start of Source Generation Time (min)	0.0	6.7	44.0	0.0
End of Source Generation Time (min)	5.75	23.7	57.0	26.0

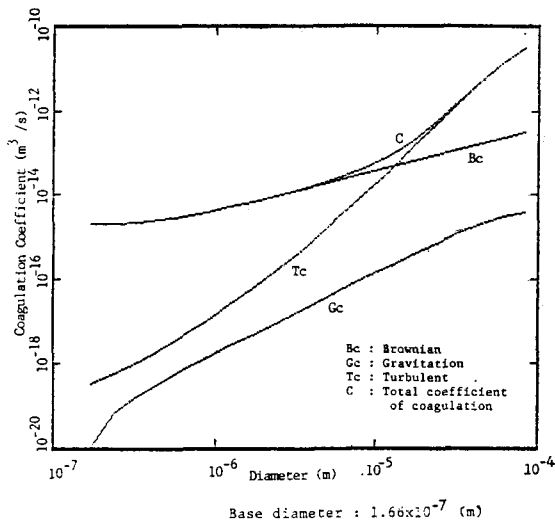


Fig. 2. Coagulation Coefficients of Three Mechanisms vs. Particle Diameter.

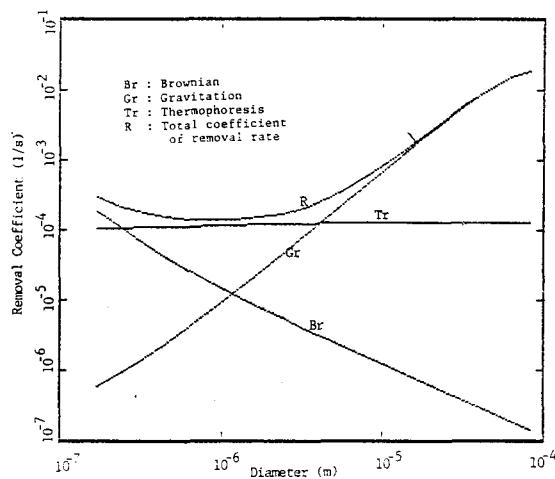


Fig. 3. Removal Coefficients of Three Mechanisms vs. Particle Diameter

coagulation. The three mechanisms of coagulation based on the diameter of 0.166 micro-meter are shown in Fig. 2. It shows the various regions where individual mechanism has its predominance. As well, removal mechanisms are shown in Fig. 3.

As compared with other multicomponent aerosol code, MCAD treats the concept of density correction and shape factors simultaneously. The gravitational and brownian coagulation have their own model based on the suggestion by

Loyalka and Fuchs respectively. The particle mass concentration as a function of time is shown in Fig. 4 and 5 and experimental results are compared. Also, there are added the result of MSPEC. These show that the MCAD fits the experimental results well.

MCAD utilizes sectionalization method which treats up to 20 sections. In Fig. 6, section number dependency of particle mass concentration is shown. This shows that, except section 5, the 10~20 sections result in a little differences. Due to the much computer time consuming, 10 section is recommended for analysis.

Sensitivity Analysis Result

MCAD developed for analysis of severe accidents in LMFBR is very uncertain in nature.

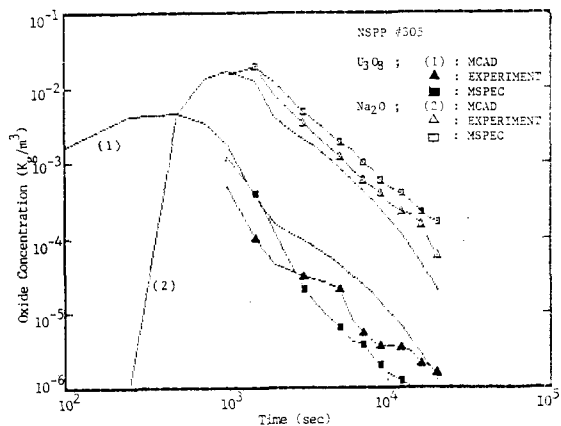


Fig. 4. Mass Concentrations of Two Component Aerosol vs. Time

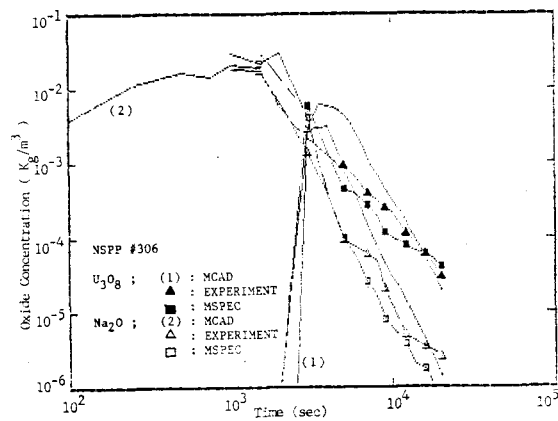


Fig. 5. Mass Concentrations of Two Component Aerosol vs. Time

Table 6. Latin Hypercube Sampling

K	N	Input Variables														Output	
		1*	2	3	4	5	6	7	8	9	10	11	12	13	14	y(1)**	y(2)
1		-1.00	-0.93	-0.85	-0.78	-0.70	-0.63	-0.56	-0.48	-0.41	-0.33	-0.26	-0.19	-0.11	-0.04	-3.384	-4.093
2		-0.93	-0.85	-0.78	-0.70	-0.63	-0.56	-0.48	-0.41	-0.33	-0.26	-0.19	-0.11	-0.04	-1.00	-3.393	-4.145
3		-0.85	-0.78	-0.70	-0.63	-0.56	-0.48	-0.41	-0.33	-0.26	-0.19	-0.11	-0.04	-1.00	-0.93	-3.560	-4.378
4		-0.78	-0.70	-0.63	-0.56	-0.48	-0.41	-0.33	-0.26	-0.19	-0.11	-0.04	-1.00	-0.93	-0.85	-3.373	-4.202
5		-0.70	-0.63	-0.56	-0.48	-0.41	-0.33	-0.26	-0.19	-0.11	-0.04	-1.00	-0.93	-0.85	-0.78	-3.302	-4.136
6		-0.63	-0.56	-0.48	-0.41	-0.33	-0.26	-0.19	-0.11	-0.04	-1.00	-0.93	-0.85	-0.78	-0.70	-3.377	-4.228
7		-0.56	-0.48	-0.41	-0.33	-0.26	-0.19	-0.11	-0.04	-1.00	-0.93	-0.85	-0.78	-0.70	-0.63	-3.452	-4.361
8		-0.48	-0.41	-0.33	-0.26	-0.19	-0.11	-0.04	-1.00	-0.93	-0.85	-0.78	-0.70	-0.63	-0.56	-3.362	-4.093
9		-0.41	-0.33	-0.26	-0.19	-0.11	-0.04	-1.00	-0.93	-0.85	-0.78	-0.70	-0.63	-0.56	-0.48	-0.520	-4.278
10		-0.33	-0.26	-0.19	-0.11	-0.04	-1.00	-0.93	-0.85	-0.78	-0.70	-0.63	-0.56	-0.48	-0.41	-3.404	-4.006
11		-0.26	-0.19	-0.11	-0.04	-1.00	-0.93	-0.85	-0.78	-0.70	-0.63	-0.56	-0.48	-0.41	-0.33	-3.699	-4.403
12		-0.19	-0.11	-0.04	-1.00	-0.93	-0.85	-0.78	-0.70	-0.63	-0.56	-0.48	-0.41	-0.33	-0.26	-3.671	-4.242
13		-0.11	-0.04	-1.00	-0.93	-0.85	-0.78	-0.70	-0.63	-0.56	-0.48	-0.41	-0.33	-0.26	-0.19	-3.733	-4.158
14		-0.04	-1.00	-0.92	-0.85	-0.78	-0.70	-0.63	-0.56	-0.48	-0.41	-0.33	-0.26	-0.19	-0.11	-3.607	-4.275
15		0.04	0.11	0.18	0.26	0.33	0.41	0.48	0.56	0.63	0.70	0.78	0.85	0.93	1.00	-4.116	-4.996
16		0.11	0.19	0.26	0.33	0.41	0.48	0.56	0.63	0.70	0.78	0.85	0.93	1.00	0.04	-4.042	-4.929
17		0.19	0.26	0.33	0.41	0.48	0.56	0.63	0.70	0.78	0.85	0.93	1.00	0.04	0.11	-4.248	-5.133
18		0.26	0.33	0.41	0.48	0.56	0.63	0.70	0.78	0.85	0.93	1.00	0.04	0.11	0.19	-4.171	-5.013
19		0.33	0.41	0.48	0.56	0.63	0.70	0.78	0.85	0.93	1.00	0.04	0.11	0.19	0.26	-4.085	-4.883
20		0.41	0.48	0.56	0.63	0.70	0.78	0.85	0.93	1.00	0.04	0.11	0.19	0.26	0.33	-4.152	-4.942
21		0.48	0.56	0.63	0.70	0.78	0.85	0.93	1.00	0.04	0.11	0.19	0.26	0.33	0.41	-4.206	-5.007
22		0.56	0.63	0.70	0.78	0.85	0.93	1.00	0.04	0.11	0.19	0.26	0.33	0.41	0.48	-4.201	-4.866
23		0.63	0.70	0.78	0.85	0.93	1.00	0.04	0.11	0.19	0.26	0.33	0.41	0.48	0.56	-4.265	-4.925
24		0.70	0.78	0.85	0.93	1.00	0.04	0.11	0.19	0.26	0.33	0.41	0.48	0.56	0.63	-4.253	-4.801
25		0.78	0.85	0.92	1.00	0.04	0.11	0.19	0.26	0.33	0.41	0.48	0.56	0.63	0.70	-4.512	-5.103
26		0.85	0.93	1.00	0.04	0.11	0.19	0.26	0.33	0.41	0.48	0.56	0.63	0.70	0.78	-4.575	-5.062
27		0.93	1.00	0.04	0.11	0.19	0.26	0.33	0.41	0.48	0.56	0.63	0.70	0.78	0.85	-4.633	-4.950
28		1.00	0.04	0.11	0.19	0.26	0.33	0.41	0.48	0.56	0.63	0.70	0.78	0.85	0.93	-4.484	-5.068

*: 1...14 is equal to the sequence of Table 4.
 **: Outputs are Log Scales of Particle concentration of U_3O_8 and Na_2O
 K=14; variable number N=28; run number

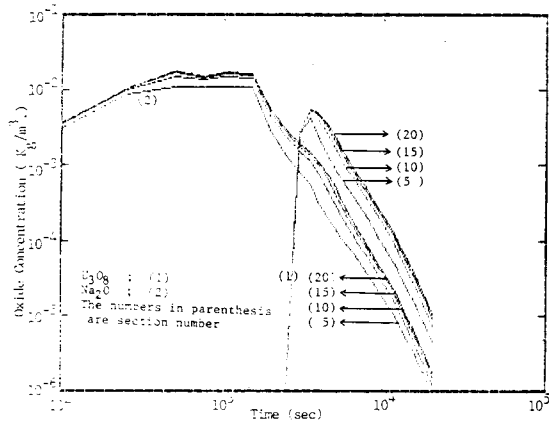


Fig. 6. Mass Concentration of Aerosol for Different Number of Sections.

The aerosol behavior model presented in section II is microphenomena in its physical behavior and parameters are not well defined. Several parameters are assumed into the code and these values are unknown sufficiently. Hence, analysis result will be discussed regarding the uncertainties of these variables.

The aerosol dynamics can be viewed as a function of time and the significance of input

variables also changes as the time elapse. To compare the results as time passes, LHS and EDM are analyzed in 1.0, 1.5, 2.0 $\times 10^4$ (sec) each other. At present, the code has not fulfilled the thermodynamic analysis. Hence, each of time values mentioned has no special meaning. But, They were stabilized time values after source being generated and sufficient time elapsed.

Computer runs of 28 and 44 are executed for the analysis of LHS and EDM each other. The assumed number of section is 10 and the data of experiment NSPP #306 are adopted. The normalized data values and outputs based on log scale of particle concentration by LHS and EDM are given in Table 6, 7.1 and 7.2.

To see the difference between Y and \hat{Y} , analysis of variance (ANOVA) are performed. Here, U_3O_8 and Na_2O are analyzed respectively and their regression models are compared. The correlation coefficients and sensitivity factors of each particle in time 10^4 sec are shown in Table 8. R^2 value which is nearly one shows the regre-

Table 7.1. Plackett-Burman Design

K	N	Input Variables														Output	
		1*	2	3	4	5	6	7	8	9	10	11	12	13	14	y(1)**	y(2)
1		+	-	+	+	-	-	-	-	+	-	+	-	+	+	-3.942	-4.686
2		+	+	-	+	+	-	-	-	-	+	-	+	-	+	-4.260	-4.128
3		-	+	+	-	+	+	-	-	-	-	+	-	+	-	-3.217	-3.961
4		-	-	+	+	-	+	+	-	-	-	-	+	-	+	-3.936	-5.357
5		+	-	-	+	+	-	+	+	-	-	-	-	+	-	-3.524	-4.107
6		+	+	-	-	+	+	-	+	+	-	-	-	-	+	-4.039	-4.112
7		+	+	+	-	-	+	+	-	+	+	-	-	-	-	-4.148	-4.286
8		+	+	+	+	-	-	+	+	-	+	+	-	-	-	-4.427	-4.853
9		-	+	+	+	+	-	-	+	+	-	+	+	-	-	-3.987	-5.014
10		+	-	+	+	+	+	-	-	+	+	-	+	+	-	-3.796	-4.616
11		-	+	-	+	+	+	+	-	-	+	+	-	+	+	-3.450	-4.288
12		+	-	+	-	+	+	+	+	-	-	+	+	-	+	-4.099	-5.140
13		-	+	-	+	-	+	+	+	+	-	-	+	+	-	-4.089	-5.359
14		-	-	+	-	+	-	+	+	+	+	-	-	+	+	-2.864	-3.608
15		-	-	-	-	-	-	-	-	-	-	-	-	-	-	-3.041	-3.570

*: ...14 is equal to the sequence of Table 4.

K=14 N=15 +=1 --=-1

** : Outputs are Log Scales

Table 7.2. Central Composite Design

K	N	Input Variables														Output	
		1*	2	3	4	5	6	7	8	9	10	11	12	13	14	y(1)**	y(2)
16		+	-4.190	-4.646
17		-	-3.622	-4.656
18		.	+	-3.934	-4.480
19		.	-	-3.681	-4.684
20		.	.	+	-3.808	-4.694
21		.	.	-	-3.795	-4.440
22		.	.	.	+	-3.901	-4.786
23		.	.	.	-	-3.681	-4.316
24		+	-3.634	-4.337
25		-	-4.043	-4.894
26		+	-3.893	-4.767
27		-	-3.665	-4.282
28		+	-3.795	-4.557
29		-	-3.869	-4.648
30		+	-3.863	-4.729
31		-	-3.698	-4.291
32		+	-3.819	-4.554
33		-	-3.789	-4.616
34		+	-3.796	-4.561
35		-	-3.812	-4.577
36		+	.	.	.	-3.938	-4.731
37		-	.	.	.	-3.669	-4.405
38		+	.	.	-3.934	-4.724
39		-	.	.	-3.560	-4.276
40		+	.	-3.718	-4.472
41		-	.	-3.925	-4.700
42		+	-3.817	-4.584
43		-	-3.786	-4.546
44		-3.712	-4.467

*: 1...14 is equal to the sequence of Table 4.

K=14 N=29 +=+1, -=-1, .=0.0

**: Outputs are Log Scales

ssion model can be substituted for computer code. This is required in case of many data are needed in Monte Carlo Method analysis or predictions are necessitated early in emergency situation.

The importance of variables is investigated by stepwise regression method. The results in Table 9 and 10 show the variation of important variable as time passes. The number of input variables selected in the sensitivity analysis is 14, but Table 9 and 10 show that the models are

regressed 98% above only using 7 input variables. This can simplify the computer code or analysis method. In these results, there is no large difference in sensitivity coefficient in each component.

Comparing the LHS and EDM, LHS shows more exact result than EDM in spite of less computer runs. In multicomponent system, which is more complicate and time consuming than two component system, LHS is more useful to analyze and is recommended.

The regression model based on full variables is quite lengthy and tedious. Hence, following simplified models are generated using the stepwise regression method;

$$Y(1) = -3.885 - 0.353 X(1) - 0.195X(2) + 0.064X(5) - 0.262 X(12) \quad (10)$$

$$Y(2) = -4.596 + 0.285 X(5) - 0.21 X(6) - 0.25 X(12) - 0.15 X(4) - 0.156 X(3) \quad (11)$$

Here, $X(1, \dots, 14)$ are normalized values of Table 4 as a sequence to their orders. Eq. (10) and (11) are based on the value of R^2 which is 97% above. The analysis must be weighed to the variables enumerated in equations.

Finally to see the uncertainty propagation of outputs of code, Monte Carlo Uncertainty Propagation²³⁾ (MOCUP) tests are executed and their results are shown in Fig. 7. The figure

Table 8. Latin Hypercube Sampling & Experimental Design Method of Each Component at 10^4 sec.

	SOURCE	Latin Hypercube Sampling					
		SS	DF	MS	F_0	$F(.05)$	R^2
U_3O_8	REGRES	5.1002	14	.36430	123.85	2.5533	.99256
	ERROR	0.0382	13	.00294			
	TOTAL	5.1384	27				
Na_2O	REGRES	4.3386	14	.30990	129.44	2.5533	.99288
	ERROR	0.0311	13	.00239			
	TOTAL	4.3697	27				
Experimental Design Method							
U_3O_8	REGRES	3.4559	14	.24685	87.68	2.0533	.97692
	ERROR	0.0816	29	.00282			
	TOTAL	3.5376	43				
Na_2O	REGRES	5.5144	14	.39389	83.27	2.0533	.97573
	ERROR	0.1372	29	.00473			
	TOTAL	5.6516	43				

SS : Sum of square due to...

DF : Degree of freedom due to...

MS : Mean square of.

. = SS/DF F_0 = MSR/MSE

$F(.05)$: Critical F value in 5% significance level

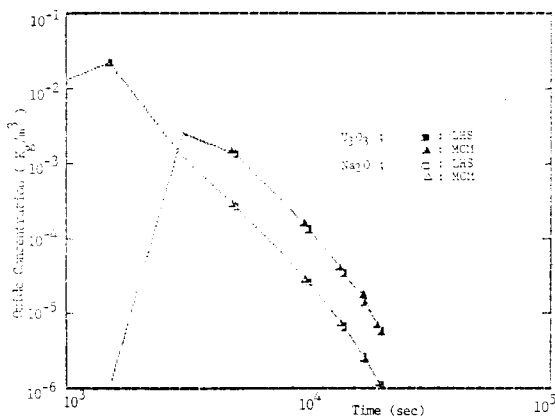
R^2 : Determination coefficient = SSR/SST

Table 9. Partial Correlation Coefficient & R^2 of First Component (U_3O_8) of Stepwise Regression Method of LHS

t	1.0×10^4			1.5×10^4			2.0×10^4		
No.	VAR.	PCC	R^2	VAR.	PCC	R^2	VAR.	PCC	R^2
1	GSD	239.7	0.902	κ	113.0	0.813	κ	135.3	0.839
2	GMD(1)	133.6	0.914	GSD	174.1	0.933	χ	66.2	0.841
3	χ	85.5	0.915	χ	137.9	0.945	Mg	42.7	0.842
4	κ	191.6	0.971	Mg	116.0	0.953	ΔT	36.5	0.864
5	ΔT	219.2	0.980	ΔT	141.7	0.970	GSD	134.9	0.968
6				GMD(1)	177.2	0.981	GMD(1)	154.4	0.978
7							Ct	135.0	0.979

Table 10. Partial Correlation Coefficient & R^2 of Second Component (Na_2O) of Stepwise Regression Method of LHS

t	1.0×10^4			1.5×10^4			2.0×10^4		
No.	VAR.	PCC	R^2	VAR.	PCC	R^2	VAR.	PCC	R^2
1	χ	38.5	0.597	χ	21.0	0.447	κ	137.6	0.841
2	α	28.7	0.697	κ	67.3	0.843	χ	66.4	0.841
3	ε	32.1	0.801	Mg	44.6	0.848	Mg	49.1	0.860
4	κ	60.6	0.913	α	47.9	0.893	ΔT	58.7	0.911
5	γ	89.1	0.953	ΔT	51.9	0.922	α	62.1	0.934
6	GMD(2)	106.7	0.968	ε	53.0	0.938	ε	61.0	0.946
7	Mg	89.2	0.969	γ	96.6	0.971	γ	104.3	0.973
8	ΔT	89.3	0.974	GMD(2)	124.8	0.981	δ	101.4	0.977
9	GSD	179.7	0.989				GMD(2)	114.0	0.983

**Fig. 7. Comparison of the Results between MCM and MCAD (Mass concentration Time Behavior of NSPP #306)**

also contains the mean values of LHS to compare these two method. These results show that two methods agree very well. Location of Fig. 7.

V. Conclusions

From this study, the conclusions are derived as follows;

- 1) The MCAD fits within 53*% deviation of the experimental results and agreed well to MSPEC.
- 2) To depict the particle shape, correction on density and shape factor are incorporated into

the model. This resulted in the shape factor 1~2 as compared to 1.3~15 of MSPEC and 1~3 of MAEROS as a actual particle shape.

3) Probabilistic concept of interaction is successfully applied to treat the two component system.

4) From the sensitivity analysis, only 4 to 5 of 14 variables turns out to have substantial weighted values above 97% of contribution to the code results. Therefore, only 5 variables of importance would suffice as a analytical study.

5) The input variables in the model have different sensitivity coefficients in each component. Hence, they must be adjusted by the significant component or the objectives of analysis.

The authors wish to recommended the following subjects.

- 1) To analyze the severe accidents of LWR, condensation mechanisms must be supplemented considering steam-air circumstances.
- 2) The containment thermodynamic analysis is required to analyze the severe accident exactly.
- 3) To see the physical health effect of source term reduction, consideration of radioactive such as Iodine and Cesium are necessary.

* Average value of percent error of each component at 1.0, 1.5, 2.0 $\times 10^4$ (sec)

References

1. Reactor Safety Study, "An Assessment of Accident of Accident Risks in the U.S. Commercial Nuclear Power Plants", (WASH-1400(NUREG-75/014), U.S. NRC (1975).
2. J.A. Gieseke et al., "Radionuclide Release Under Specific LWR Accident Conditions", BMI-2104 (Vol. IV), (1984).
3. ANS, "Report of the Special Committee on Source Terms", (1984).
4. IAEA, "Source Term Evaluation for Accident Conditions: Proceedings of a Symposium", (1985).
5. J.A. Gieseke, K.W. Lee et al., "HAARM-3 code verification procedure", NUREG/CR-3077, (1982).
6. H. Jordan et al., "Modeling of Multi-component Aerosols-Sensitivities to Assumptions", Nuc. Tech., Vol. 72(148), (1986).
7. J.C. Helton et al., "Uncertainty and Sensitivity Analysis of a Model for Multicomponent Aerosol Dynamics", Nuc. Tech., Vol. 73(320), (1986).
8. F. Gelbard, Y. Tambour and J.H. Seinfeld, "Sectional Representations for Simulating Aerosol Dynamics", J. Colloid Interface Sci., Vol. 76(541), (1980).
9. F. Gelbard and J.H. Seinfeld, "Simulation of Multicomponent Aerosol Dynamics", J. Colloid Interface Sci., Vol. 78(485), (1980).
10. R.E. Adams et al., "Uranium Oxide and Sodium Oxide Aerosol Experiments: NSPP Mixed Oxide Tests 303-307.", NUREG/CR-2697, (1982).
11. G. Narsimhan and E. Ruckenstein, "The Brownian Coagulation of Aerosols Over the Entire Range of Knudsen Number: Connection Between the Sticking Probability and Interaction Forces", J. Colloid Interface Sci., Vol. 104(344), (1985).
12. G. Zebel, "Aerosol Science", Academic Press, Chap. 2(31), (1966).
13. M. Sitarski and J.H. Seinfeld, "Brownian Coagulation in the Transition Regime", J. Colloid Interface Sci., Vol. 61(261), (1977).
14. G.A. Pertmer and S.K. Loyalka, "Gravitational Collision Efficiency of Post-HCDA LMFBR Aerosols: Spherical particles", Nuc. Tech., Vol. 47(70), (1980).
15. R.F. Tuttle and S.K. Loyalka, "Gravitational Agglomeration of Post-HCDA LMFBR Aerosols: Nonspherical particles", NUREG/CR-3029, (1982).
16. P.G. Saffman and J.S. Turner, "On the Collision of Drops in Turbulent Clouds", J. Fluid Mech., Vol. 1(16), (1956).
17. Thomas T. Mercer, "Aerosol Technology in Hazard Evaluation", Academic Press, Chap. 3(65), (1973).
18. B. Carnahan et al., "Applied Numerical Methods", Chap. 6(341), John Wiley and Sons, Inc, (1969).
19. Jack. P.C. Kleijnen, "Statistical Techniques in Simulation", Part II, Chap. IV(287), Marcel Dekker, (1984).
20. R.L. Iman and W.J. Conover, "Small Sample Sensitivity Analysis Techniques for Computer Model, With an Application to Risk Assessment", Comm. Stat., A9, (1749), (1980).
21. R.M. Mayers, "Response Surface Methodology", Allan and Bacon, Inc., (126), (1976).
22. R.L. Iman, J.C. Helton and J.E. Campbell, "An Approach to Sensitivity Analysis of Computer Models: Part 1-Introduction, Input Variable Selection and Preliminary Variable Assessment", J. Quality Tec., Vol. 13(174), (1981).
23. T.W. Kim and S.H. Chang, "MOCUP: Monte Carlo Uncertainty Propagation Program", KAIST, Nuclear Eng. Dept., (1985).